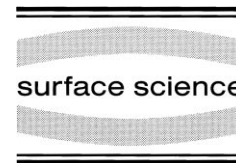




ELSEVIER

Surface Science 423 (1999) 70–84



GaN(0001) surface structures studied using scanning tunneling microscopy and first-principles total energy calculations

A.R. Smith ^a, R.M. Feenstra ^{a,*}, D.W. Greve ^b, M.-S. Shin ^c, M. Skowronski ^c,
J. Neugebauer ^d, J.E. Northrup ^e

^a Department of Physics, Carnegie Mellon University, Pittsburgh, PA 15213, USA

^b Department of Electrical and Computer Engineering, Carnegie Mellon University, Pittsburgh, PA 15213, USA

^c Department of Materials Science and Engineering, Carnegie Mellon University, Pittsburgh, PA 15213, USA

^d Fritz-Haber-Institut der Max-Planck-Gesellschaft, Faradayweg 4–6, D-14195 Berlin, Germany

^e Xerox Palo Alto Research Center, 3333 Coyote Hill Road, Palo Alto, CA 94304, USA

Received 16 September 1998; accepted for publication 24 November 1998

Abstract

Surface reconstructions occurring on the (0001) surface of wurtzite GaN are studied using scanning tunneling microscopy, electron diffraction, and Auger electron spectroscopy. The family of reconstructions found on this face includes 2×2 , 5×5 , 6×4 , and 1×1 , in order of increasing surface Ga/N ratio. Detailed experimental results are presented for each of these reconstructions. First-principles total energy calculations are employed to identify possible model structures. An adatom model, with N-adatoms occupying H3 sites, is proposed for the 2×2 reconstruction. A model composed of N adatoms, Ga adatoms, and Ga vacancies is proposed for the 5×5 reconstruction. © 1999 Elsevier Science B.V. All rights reserved.

Keywords: Density functional calculations; Gallium nitride; Low-index single crystal surface; Reflection high-energy electron diffraction (RHEED); Scanning tunneling microscopy; Surface reconstruction

1. Introduction

A large amount of research has been aimed at studying both the structural and electronic properties of wurtzite GaN surfaces. Several prior studies have reported that these surfaces do not reconstruct, as compared to the more traditional and analogous III–V semiconductor surfaces such as GaAs(111)A and (111)B, both of which exhibit a number of reconstructions, depending on the surface stoichiometry [1–3]. However, a variety of

diffraction symmetries other than 1×1 have been reported, but the nature of these reconstructions was completely unknown [4–10]. Recently, however, two classes of surface reconstructions were identified, corresponding to the two inequivalent polar faces of wurtzite GaN, the (0001) or Ga face, and the $(000\bar{1})$ or N face [11,12]. Scanning tunneling microscopy (STM), reflection high energy electron diffraction (RHEED), and theoretical total energy calculations were all essential in the classification of these reconstructions. Those occurring on the N face, 1×1 , 3×3 , 6×6 , and $c(6 \times 12)$, have already been described in detail

* Corresponding author.

[13,14]. In this article, we discuss the reconstructions occurring on the Ga face, which include 2×2 , 5×5 , 6×4 , and $'1 \times 1'$ (pseudo- 1×1), listed in order of increasing surface Ga concentration. In the section on $'1 \times 1'$ (Section 3.4), we introduce in addition a fifth and especially novel reconstruction which we conclude has 5.08×2.54 -R20° symmetry. The theory section (Section 4) forming the latter part of the paper describes in detail model structures for the 2×2 and 5×5 . Finally, while this paper is meant to provide a comprehensive discussion of all the Ga-face reconstructions, we also refer the reader to two additional papers that focus particularly on the 2×2 and $'1 \times 1'$ reconstructions [15,16].

2. Experimental

These experiments are performed in a combination growth and analysis system. Samples are prepared by MBE using an r.f. plasma source to activate the N_2 molecules. When GaN growth is initiated directly on sapphire substrates, as described in detail elsewhere [13], the film is found to be N-polar (the surface is N face). However, smooth GaN films grown by metal organic chemical vapor deposition (MOCVD) have been found to be Ga-polar (surface is Ga face) [17–19]. To prepare the Ga-face reconstructions, therefore, we use an MOCVD-grown GaN/sapphire film as an atomic-scale template. This template is first cleaned with solvents and then loaded into the MBE chamber where it is exposed to a nitrogen plasma at the typical growth temperature of 750°C for about 5 min prior to opening the Ga shutter to begin the GaN growth. In order to study the surface reconstructions using STM, we find it necessary to dope the film with Si. The doping is stopped a few minutes prior to terminating the film growth, after which the various reconstructions are prepared on the fresh surface, as described below. Samples ready for investigation are transferred through a UHV gate valve into the adjoining analysis chamber, which includes STM, low energy electron diffraction (LEED) and Auger electron spectroscopy (AES). The base pressure in the analysis chamber is 6×10^{-11} Torr. STM images were acquired with a constant tunnel cur-

rent of 0.075 nA and at various sample voltages specified below.

We prepared the 2×2 reconstruction by nitriding the Ga face at about 600°C [11,12]. The 5×5 reconstruction is obtained by annealing the Ga face at 750°C , depositing 1/2 ML of Ga, then re-annealing the surface to about 700°C . The surface obtained by annealing at 750°C alone is found to be disordered, but the Ga deposition and re-annealing process stabilizes the surface via the 5×5 reconstruction. The 6×4 is formed by deposited 1/2 ML of Ga on to the 5×5 and then briefly heating the surface up to 700°C . Ga deposition alone will not produce the 6×4 , suggesting that the formation of the 6×4 must involve extensive rearrangement of surface atoms. Surfaces showing clear 6×4 RHEED patterns obtained in this manner, however, are also found to contain large domains of 5×5 , as shown in Fig. 1 below. The $'1 \times 1'$ structure can be formed in several ways, one of which is by depositing about 1 ML of Ga on to the 6×4 , followed by a rapid anneal to 700°C . Another way to form the $'1 \times 1'$ is to terminate the growth of GaN under slightly Ga-rich growth conditions. As in the sample cools, the entire surface can become $'1 \times 1'$, although 5×5 and 6×4 may also be observed, depending on the precise amount of Ga present on the surface.

3. Results and discussion

We find that atomically flat, reconstructed surfaces are common for the Ga face just as they are for the N face [12]. This is illustrated in Fig. 1, where three adjacent terraces are observed, separated by single bilayer-height steps. This image also illustrates 5×5 and 6×4 reconstructions co-existing on the same surface. In this image, both 5×5 and 6×4 are observed on the upper terrace (at left), 6×4 on the middle terrace, and 5×5 on the lower terrace. The 6×4 is a fairly well-ordered, row-like structure, resulting in the appearance of different rotational domains, illustrated in Fig. 1 as R1, R2 and R3. While the 5×5 does not show such large domains, it does turn out to be an ordered structure, as discussed below.

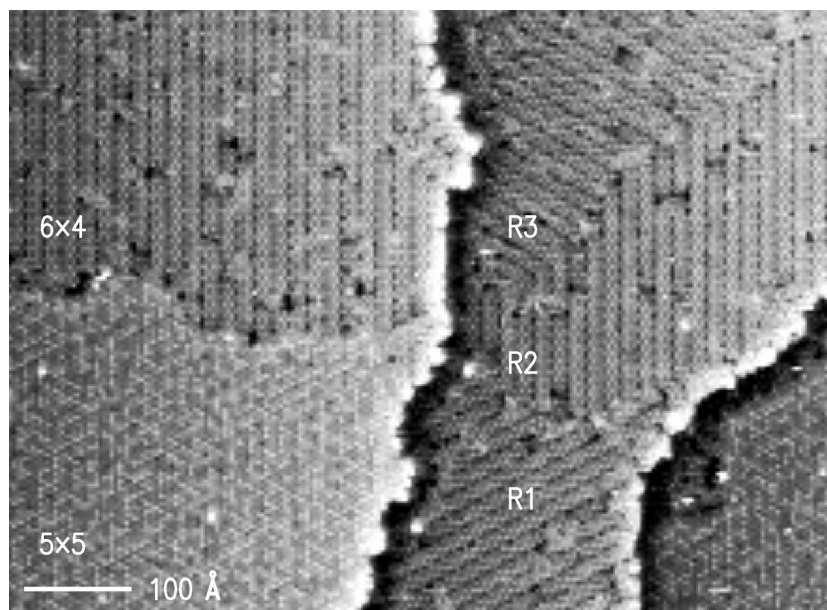


Fig. 1. STM image of Ga face showing 5×5 and 6×4 reconstructions. The three terraces are separated by single bilayer-height steps (1 bilayer = 2.59 \AA). R1, R2, and R3 indicate three different rotational domains of the row-like 6×4 reconstruction. Sample bias = -1 V ; tunnel current = 0.075 nA . The image is displayed with a local area background subtraction.

We have performed AES on all of the surface reconstructions for both the Ga face and the N face [16]. Results for just the Ga-face reconstructions are shown in Fig. 2 where the Ga/N Auger intensity ratio is plotted for the different reconstructions. The scale on the right is the corresponding number of Ga monolayers on top of the Ga-terminated bilayer, based on a computation of Auger intensity ratios [16]. The Ga/N Auger ratios

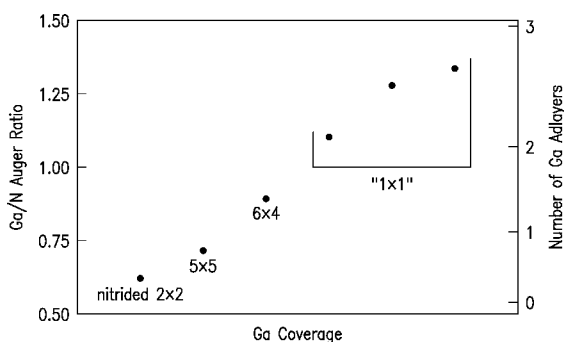


Fig. 2. Ga/N Auger intensity ratios for various reconstructions on the Ga face. The scale on the right shows the corresponding number of Ga adlayers, derived from a numerical simulation of Auger intensities.

for the Ga-face reconstructions show a wide variation. The 5×5 and 6×4 reconstructions have ratios in the range of 0.7–0.9. The nitrated 2×2 has a slightly smaller ratio, and the three different ' 1×1 ' surfaces have much larger ratios. Although we do not consider these data for Auger ratios to be a completely reliable predictor of surface stoichiometry, the qualitative ordering of Ga surface coverage shown in Fig. 2 does provide some guidance in determining structural models.

3.1. 2×2 reconstruction

Fig. 3 shows an STM image of the 2×2 reconstruction, prepared by nitrating the Ga face at about 600°C . This image was acquired at negative sample bias. Imaging at positive sample bias was not successful, suggesting a semiconducting surface. Not surprisingly, much of the surface is disordered, consistent with the fact that the $\frac{1}{2}$ -order diffraction lines seen in RHEED are not very sharp [12]. However, small domains of well-ordered 2×2 reconstruction are seen throughout the image. From the total energy calculations for the Ga face,

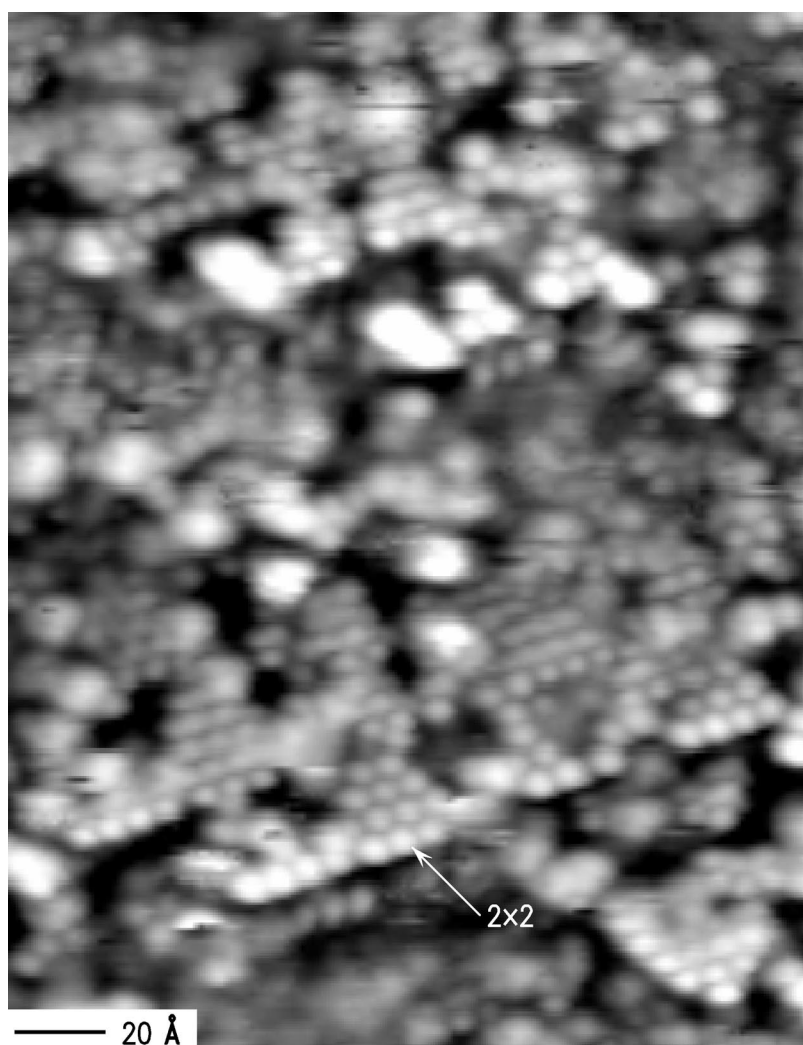


Fig. 3. STM image of nitrided surface showing small ordered areas of 2×2 reconstruction. Sample bias = -2.0 V; tunnel current = 0.075 nA; gray scale range = 3.0 Å.

two different 2×2 structures are found to be energetically favorable within a certain range of the allowed Ga chemical potential: the N adatom (T4) 2×2 [13]. The fact that this 2×2 is formed by nitridation suggests that what we observe is the N adatom 2×2 . In terms of Ga/N Auger ratios, we expect values of 0.52 for the N adatom 2×2 and 0.62 for the Ga adatom 2×2 . The observed value is 0.62 , as shown in Fig. 2, suggesting the possibility of the Ga adatom 2×2 . However, since much of our nitrided 2×2 surface is clearly not

well-ordered, we consider it unreliable to determine its stoichiometry from these Auger measurements.

Besides forming the 2×2 by nitridation, we have found a second method for producing at 2×2 on the Ga face [11]. This method requires first preparing the 5×5 reconstruction, as described below, and then slowly heating this 5×5 until the $\frac{1}{2}$ -order diffraction lines disappear. After cooling the sample, weak $\frac{1}{2}$ -order diffraction lines are observed. STM imaging of such a surface, however, shows only small remnant patches of

5×5 surrounded by disordered regions. Since these disordered regions comprise most of the surface, it is difficult to locate any ordered 2×2 domains. Consequently, we do not know whether the 2×2 prepared by annealing the 5×5 is the same structure as that prepared by nitridation.

As discussed elsewhere [15], a number of authors have reported stable 2×2 reconstructions during MBE growth of GaN. However, we have failed to obtain such a RHEED pattern during growth despite an extensive search using different growth temperatures and nitrogen sources [15]. We can obtain a 2×2 pattern by interrupting the Ga flux during growth, but not during steady state growth conditions. For this reason, we have suggested that the 2×2 arrangements observed during growth by other groups may be of extrinsic origin, involving the presence of unintentional atoms, such as As or Mg, in the growth chamber [15].

3.2. 5×5 reconstruction

Compared to reconstructions found on the N face, the Ga face 5×5 is strongly bias-dependent, suggestive of a semiconducting surface. Shown in Fig. 4 is a pair of STM images of the 5×5 reconstruction acquired at positive sample bias (empty states) in (a), and negative sample bias (filled states) in (b), from nearby surface locations. At a positive sample bias, the unit cells of the 5×5 can be readily identified by the dark trenches traversing

the image in all three of the $\langle 11\bar{2}0 \rangle$ directions. One 5×5 unit cell is marked in the image. Typically, four topographic maxima are observed within each unit cell. However, the height and shape of these maxima vary from one unit cell to the next. This lack of translational equivalence is even more evident at negative sample bias, when the topographic maxima appear to be grouped together on the surface into pairs, or in some cases, triplets. The more common pair features have a specific rotational orientation, namely along one of the $\langle 11\bar{2}0 \rangle$ directions, with the particular orientation varying randomly over the surface.

To understand the symmetry of the 5×5 , it is useful to analyze simultaneously acquired dual bias data, as shown in Fig. 5. First, a triangular 5×5 lattice is overlaid on the both images, dividing each unit cell into two triangular halves. The lattice is adjusted such that the vertices coincide with topographic maxima seen at positive sample bias. Since these maxima lie at the corners of the unit cell, they comprise just one out of the four maxima per unit cell. The maxima on the edges of the unit cell comprise two out of the four, and the fourth maximum lies near the center of the unit cell. Two of the four maxima also appear at a negative sample bias as a pair, always on the same half of the unit cell.

The exact atomic registry of the four maxima is determined by overlaying the two images with primitive 1×1 lattices. The results are synthesized

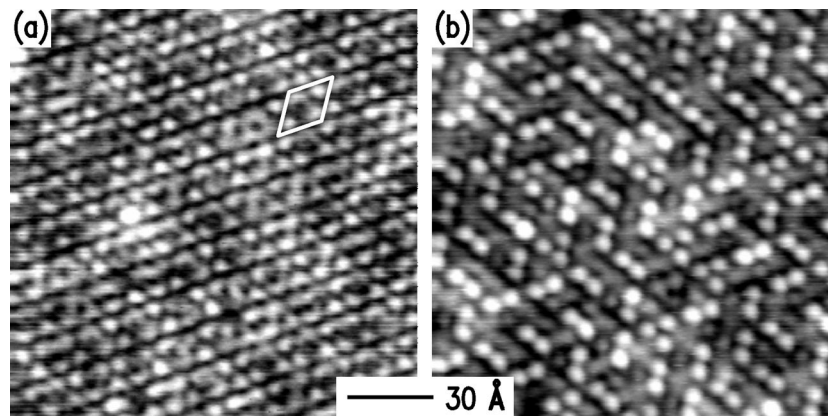


Fig. 4. Simultaneously acquired dual bias images of the 5×5 reconstruction. Sample biases are $+1.0$ V and -1.0 V with gray scale ranges of 0.5 Å and 0.9 Å for (a) and (b), respectively.

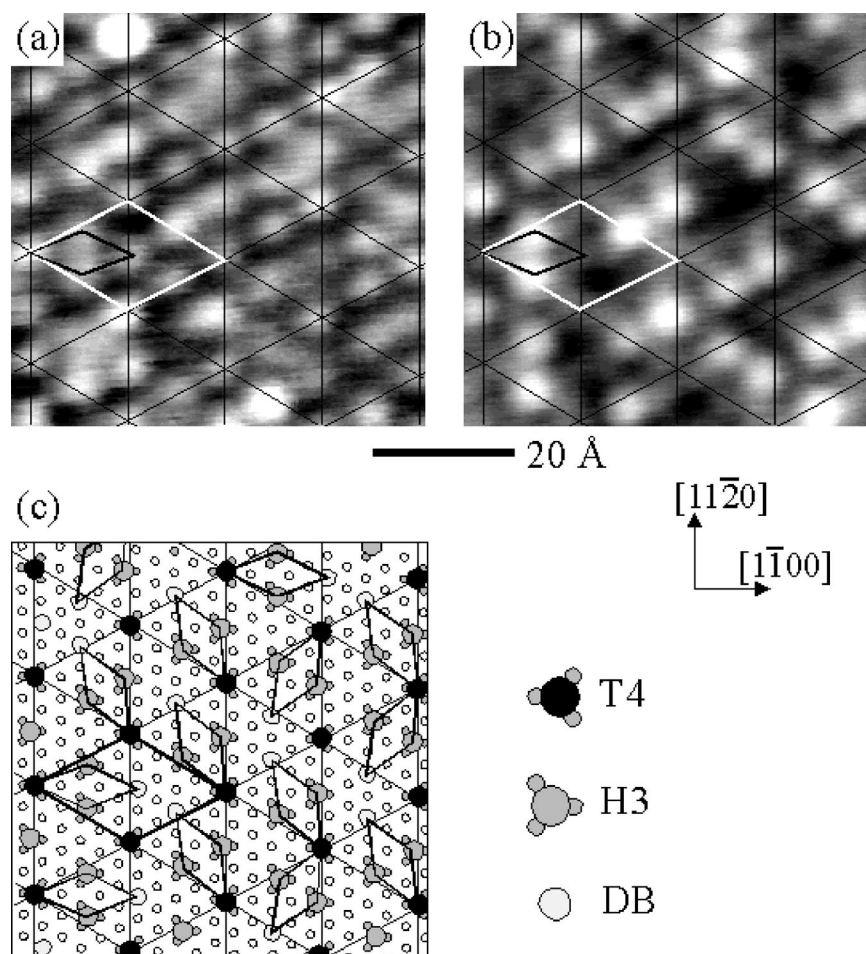


Fig. 5. Simultaneously-acquired dual bias images of the 5×5 reconstruction. Sample biases are +2.0 and -2.0 V with gray scale ranges of 0.5 and 0.6 Å for (a) and (b), respectively. A 5×5 grid is superimposed on each image with the corners located on the bright features seen in (a). Shown in (c) is the same 5×5 grid where the underlying primitive lattice is shown in empty circles. Black circles are T4 adatom sites. Dark-gray circles are H3 adatom sites. Light-gray circles are DB (dangling bond) sites. The small diamond shapes represent the basic structural unit for the 5×5 , which is found in three possible orientations throughout the surface.

into a single schematic diagram, shown in Fig. 5c. If the maxima at the corners of the 5×5 units cells correspond to T4 sites, then the maxima of the pair features correspond to H3 sites. The one remaining maximum per unit cell is then a DB (dangling bond) site. One can now define the basic structural unit for each unit cell of the 5×5 as one T4 site, one pair of H3 sites, and one DB site (shown connected by the small diamond shape). As can be seen from Fig. 5c, the surface is composed entirely of these structural units. Since the rotational orientation of these units varies ran-

domly across the surface, the largest single 5×5 domain is only a few unit cells in size. We should note that different site assignments to those given above can be derived by shifting the lattice overlays. For example, if the overlays are shifted by $\frac{2}{3}a$ along a $[1\bar{1}00]$ direction, the T4 site becomes the DB site, the H3 site becomes the T4 site, and the DB site becomes the H3 site. In terms of specific structural models, the results in Fig. 5c are very suggestive of adatoms (in H3 and T4 sites) of the surface, with three adatoms per 5×5 unit cell. The DB site is located at a Ga rest atom, although

position of this corrugation maxima could also conceivably be consistent with an additional adatom (H3 or T4) in each unit cell. Such a sparse arrangement of adatoms (three or four per 5×5 cell) implies the existence of additional structural units, such as vacancies. Also, some such additional structural unit is required to satisfy electron counting. Possible structural models for the 5×5 are further discussed in Section 4.

3.3. 6×4 reconstruction

Fig. 6 shows high-resolution views of the upper terrace of the surface shown in Fig. 1 at both positive sample bias and negative sample bias. As with the 5×5 , the row-like 6×4 structure shows a strong bias dependence, again suggesting a semi-conducting surface. At a positive sample bias, each row is clearly defined by a line of bright features spaced $4 \times a$ ($a = 3.19 \text{ \AA}$) apart along the $[11\bar{2}0]$ direction, except where a structural defect breaks the periodicity. At negative sample bias, these

maxima do not appear, but the rows are still clearly defined by a line of dark features having the same $4 \times$ spacing.

Although the 6×4 forms large rotational domains, within these domains, there is often a variation in the local symmetry. For example, consider two adjacent rows of this structure. The spacing between the rows is $6 \times (\sqrt{3}/2) \times a$, whereas the spacing between features along the row is $4 \times a$. The consistency of these spacings results in a clear 6×4 RHEED pattern. However, a local domain of true 6×4 reconstruction only occurs if the second row is shifted relative to the first by an odd number $m \times a$. If the second row is shifted relative to the first by an even number $n \times a$, then a different local symmetry will occur.

One can also see from Fig. 6 that the 6×4 appears topographically *lower*, on average, than the 5×5 . This is counter-intuitive since the 6×4 is formed by *adding* Ga to the 5×5 . One possible explanation is that the height difference is electronic in nature. However, this seems insuffi-

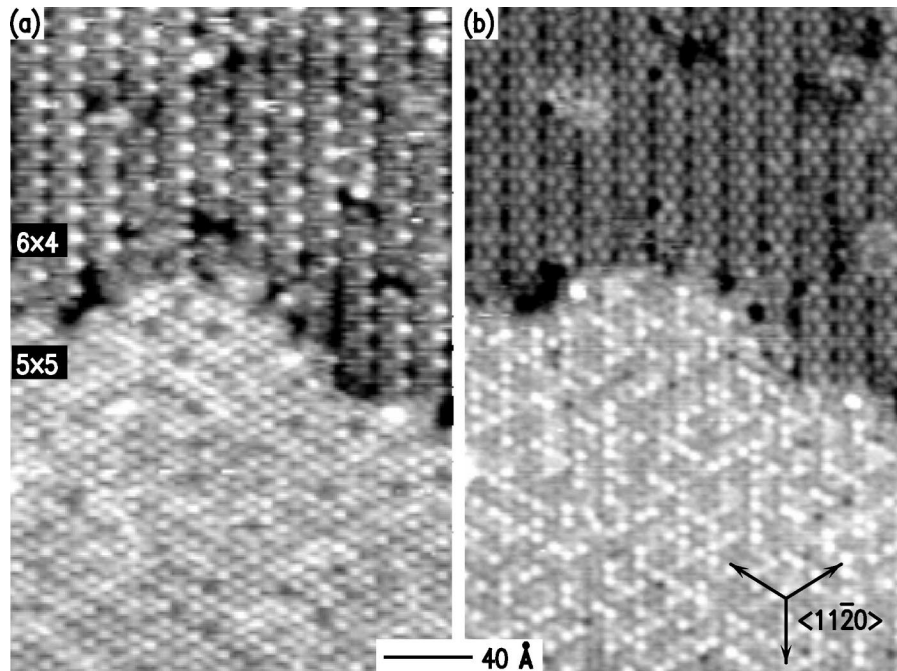


Fig. 6. Dual bias images of the 5×5 and 6×4 reconstructions. The average height difference between the two reconstructions is 0.3 \AA for empty states ($+1.0 \text{ V}$ sample voltage) shown in (a) and 0.4 \AA for filled states (-1.0 V sample voltage) shown in (b), with the 5×5 being higher in each case. In both images, the total gray scale range is about 1.3 \AA .

cient to explain the difference since the 5×5 is higher than the 6×4 at *both* positive sample bias (by 0.3 Å) and negative sample bias (by 0.4 Å). A second possibility is based on our observation, shown below, that 6×4 surfaces contain not only 5×5 but also 1×1 . This latter structure is known to contain much more Ga compared to the other reconstructions, as measured by AES. The fact that all three reconstructions are found together suggests that the 5×5 and 6×4 may not be very different from each other in terms of energy, and possibly also Ga coverage. The 1×1 , however, might be energetically much more favorable, effectively acting as a Ga ‘sink’. In any case, it is hard to imagine that the 6×4 could contain *less* Ga than the 5×5 . The additional Ga in the 6×4 could form a structural arrangement allowing denser packing of Ga compared to the 5×5 . The observed height difference might then be explained by a combination of both structural and electronic effects. We return to this point in Section 4.

Fig. 7 illustrates the bias dependence of the 6×4 ; each pair of images is acquired simultaneously at opposite biases. Images are shown with positive sample bias on the left and negative sample bias on the right. From top to bottom, the images are shown as a function of decreasing bias magnitude. At larger biases, the single bright maxima are the dominant features at positive sample bias; these features become weaker with decreasing bias. (There is a slight elongation of the bright maxima seen in empty states. This is apparently due to a small tip asymmetry but does not introduce any major artifact into the data.) As they become weaker, a ring-like structure appears for every unit cell, and at the lowest bias (0.5 V), only the features comprising this ring structure are visible. At negative sample bias, there is not as much voltage-dependence; however, more structure is evident, and at the lowest bias, the image is very similar to the corresponding image at positive sample bias.

Structural models for the 6×4 must take into account this strong bias dependence. Fig. 8 shows another pair of simultaneously acquired dual bias images of the 6×4 , where the resolution is somewhat better compared to the images shown in Fig. 7. Additionally, this local area has almost

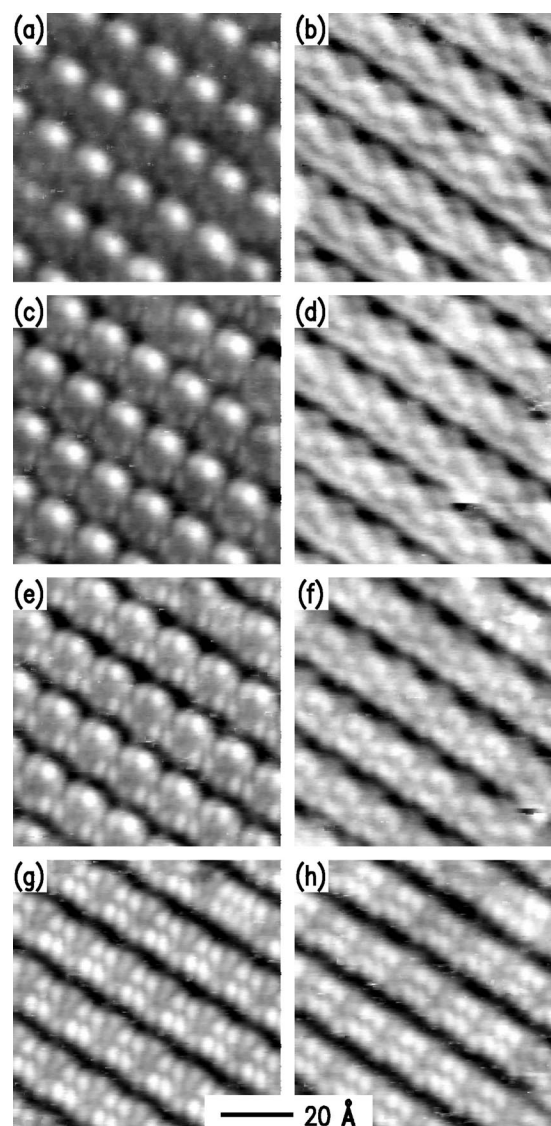


Fig. 7. Simultaneously acquired dual bias images of the 6×4 reconstruction. Sample biases are +2.0 and -2.0 V for (a) and (b), +1.5 and -1.5 V for (c) and (d), +1.0 and -1.0 V for (e) and (f), and +0.5 and -0.5 V for (g) and (h), respectively. Similarly, gray-scale ranges are 1.1 and 0.7 Å for (a) and (b), 1.1 and 0.8 Å for (c) and (d), 1.1 and 0.9 Å for (e) and (f), and 1.3 and 1.3 Å for (g) and (h).

perfect 6×4 symmetry. The ring-like structures seen at positive sample bias are reminiscent of the ring structures of the 6×6 reconstruction on the N face [14]. However, the N face 6×6 ring structures appear at both biases, indicating a metallic

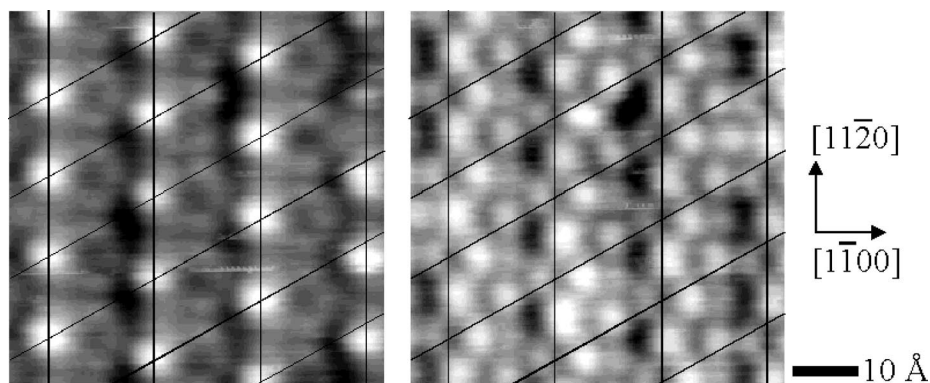


Fig. 8. Simultaneously acquired dual bias images of the 6×4 reconstruction overlaid with 6×4 grids. Sample biases and gray-scale ranges are $+1.0$ V and 1.2 Å for (a) (left) and -1.0 V and 0.8 Å for (b) (right).

surface. In the case here of the 6×4 , images at opposite biases look completely different, with no sign of ring structures at negative sample bias. Moreover, we note by overlaying a 6×4 grid on the image that maxima at a positive sample bias correlate with minima at a negative sample bias, and vice versa. For a semiconducting surface, as this 6×4 seems to be, we expect that the electron counting rule will be followed fairly closely. It is clear that the basic structural unit that comprises the 6×4 structure is quite complicated, likely involving more than simply adatoms and/or vacancies on the surface. At this time, we do not offer any specific structural model for this reconstruction.

3.4. '1 × 1' reconstruction

The '1 × 1' reconstruction, with quotation marks, is so called because of the fact that it is not a true 1 × 1 for a number of reasons, which have been discussed previously [11,12,16]. This reconstruction is the most Ga-rich structure occurring on the Ga face. Using the preparation procedures described in Section 2, we often find regions of '1 × 1' co-existing with 5×5 and 6×4 , as shown in Fig. 9. Three adjacent terraces are displayed there using a split gray scale that brings out the details of the features on each terrace. The lowest terrace, at left and top center of the image, contains both 5×5 and 6×4 . This lower terrace is delineated from the middle terrace, which is all

6×4 , by the meandering black and white boundary (a result of the split gray scale display), which marks the location of the step edge. The height of this step measures 2.6 Å, so it is a single bilayer step. The somewhat heavier black and white boundary marks the location of the step separating the middle terrace from the upper terrace. The upper terrace is '1 × 1'. The height of the step up from 6×4 to '1 × 1' measures 4.6 Å, which is equal to one bilayer (2.6 Å) plus 2.0 Å. The extra 2.0 Å is the difference between the 6×4 and the '1 × 1' if they were both on the same terrace. Such '1 × 1' domains surrounded by 6×4 on the same terrace have been found, and their step height agrees very well with this value [16].

In a previous paper, we demonstrated that the '1 × 1' consists of a double layer of Ga on top of the Ga-terminated bilayer [16]. This conclusion was based on STM, LEED, RHEED, and AES measurements as well as theoretical calculations. One of the key aspects of the '1 × 1' is that satellite peaks split off from the integral order peaks are observed in diffraction. Such peaks are suggestive of a discommensurate surface structure. High-resolution STM measurements on this '1 × 1' surface, however, do not reveal a contracted lattice but rather one whose spacing is in agreement with the surface lattice constant of GaN (3.19 Å). The explanation for these two disparate observations is that the '1 × 1' is in a fluid-like state at room temperature so that the STM measurements (which were done at room temperature) yield the lattice

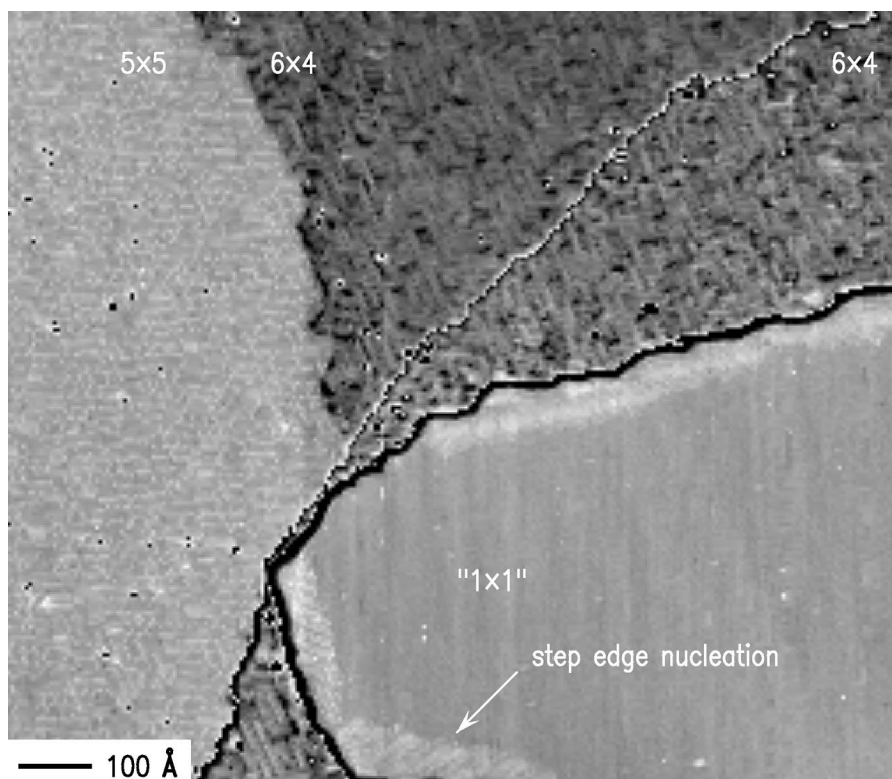


Fig. 9. STM image of Ga face showing 5×5 , 6×4 , and 1×1 reconstructions on three different terraces. The image is displayed with split gray scales to bring out the contrast on each terrace. The lowest terrace has both 5×5 and 6×4 domains. A single bilayer step running approximately from lower left to upper right separates the lowest terrace (at left) from the middle terrace, which is 6×4 . The upper terrace (at lower right) is all 1×1 except near the step edges, where a different reconstruction appears. The gray scale ranges are 2.2, 1.4, and 1.4 Å for the lowest, middle, and upper terraces, respectively, with step height differences of 2.6 Å between the lowest and middle terraces and 4.6 Å between the middle and upper terraces. The sample bias is -1.5 V.

spacing of the underlying Ga-terminated bilayer due to an averaging effect while the diffraction sees also the contracted layer [16].

While STM images of the 1×1 typically appear featureless (except at very high resolution), it is not uncommon to observe small domains of a different reconstruction near the edges of the 1×1 domains. Such features are clearly observable on the upper terrace of the image shown in Fig. 9. Unfortunately, there is not enough reconstruction present in this image to permit its identification. Occasionally, however, we find larger domains. An example of this is shown in Fig. 10, which is a high-resolution view of a reconstruction found on an otherwise 1×1 terrace. In this STM image, we observe two separate rotational domains

of a very well-ordered reconstruction. The reconstruction appears as rows of pairs of bright maxima. It is straightforward to draw the unit cell for this reconstruction; this unit cell is indicated on the image. Next, the size of the unit cell is measured. The long side measures $5.08a$, where $a = 3.19$ Å is the GaN lattice constant, and the short side measures $2.54a$. Since a 5.08×2.54 reconstruction is not related in any simple way to the underlying GaN surface unit cell, one possibility is that the lateral length calibration of the STM is in error. For example, if the calculation constant were 18% too large, then this reconstruction would measure 6×3 . However, the lateral calibration for this particular STM tip is known to within less than 2% by means of a separate

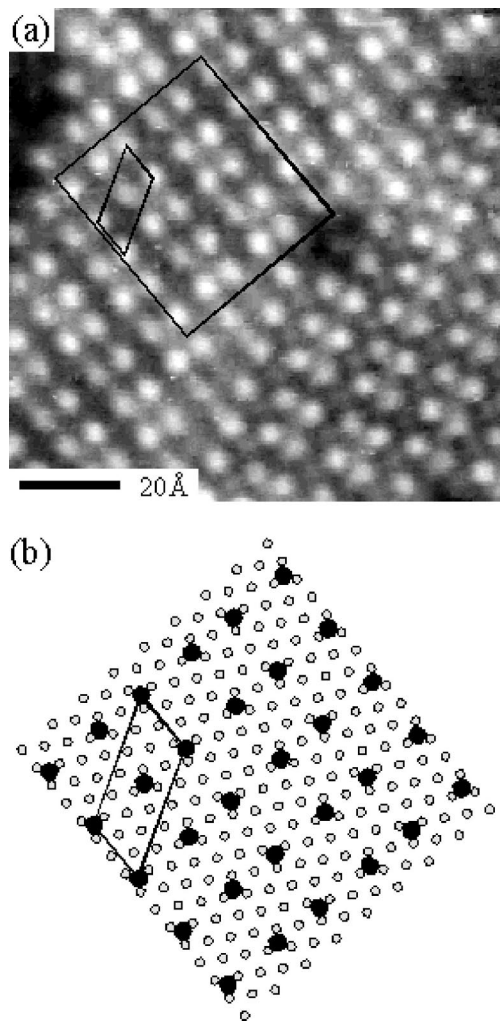


Fig. 10. (a) STM image of two rotational domains of the $5.08 \times 2.54\text{-R}20^\circ$ reconstruction found on a 1×1 area. The sample bias is $+1.0$ V and the gray-scale range is 0.7 Å. (b) Schematic adatom model of the reconstruction shown in (a). Unit cells are indicated in both image and model.

atomic scale calibration (The lateral calibration of the STM depends on the length of the probe tip, due to the bending motion of the tube scanner.)

There is one other intriguing explanation for the observed unit cell size. The diffraction results suggest, as mentioned previously, that the 1×1 is a discommensurate structure consisting of a laterally contracted double layer of Ga. The amount of lateral contraction is based on the positions of the split-off peaks seen in the diffrac-

tion pattern and is about 16% compared to the lattice constant of GaN. This value indicates that the double layer of Ga contracts to achieve an interatomic separation close to that of atoms in bulk Ga metal: about $2.7\text{--}2.8$ Å. In fact, calculations performed for a free-standing hexagonal Ga bilayer as a function of the hexagonal lattice constant predict a minimum formation energy for lattice constant of 2.7 Å [16]. Thus, the equilibrium in-plane spacing of a Ga bilayer bonded to the Ga face may be reduced from the ideal value (3.19 Å) by as much as 16%. We note that, on the N face, the 1×1 Ga adlayer does not contract laterally from the ideal separation because this would necessitate a weakening of the very strong N–Ga bonds between the Ga adlayer and the N atoms. However, in the case of the 1×1 structure on the Ga face, the surface atoms *do* contract laterally because the bonding between the Ga adlayer and the Ga atoms in the substrate is somewhat weaker. Assuming this model of a contracted double layer is correct, then the reconstruction we observe in Fig. 10 agrees very well with a 6×3 , relative to this contracted layer. By comparing this reconstructed area to the surrounding regions of 6×4 , we find that the high-symmetry directions for the reconstruction are rotated by about 20° relative to the high-symmetry directions of the GaN. Such a rotation is not unlikely since discommensurate overlayers are well-known to have their lattices rotated relative to the substrate lattice. Thus, this reconstruction may be referred to as $5.08 \times 2.54\text{-R}20^\circ$.

Having found a plausible explanation for the symmetry of this reconstruction, the next step is to identify a possible model structure and to understand the relationship of this structure to the fluid-like 1×1 . One possibility is that this $5.08 \times 2.54\text{-R}20^\circ$ reconstruction is just the 1×1 slightly below its phase transition temperature, i.e. when it transforms into a static, ordered state. Since the melting point of bulk Ga metal is 29.8°C , it is possible that the 1×1 is near such a transition at room temperature. It is also possible that the freezing-in process could begin at step-edges, which would agree with the STM image of the 1×1 terrace in Fig. 9. Another possibility is that the

fluid-like ‘1 × 1’ is somehow stabilized by additional Ga adatoms. Shown in Fig. 10b is a very simple adatom model, which agrees quite well with the STM image of Fig. 10a. In the framework of the rotated (by 20°) and contracted ‘1 × 1’ lattice (shown in empty circles), the Ga adatoms in this model sit on every third site along both the $[11\bar{2}0]$ and $[1\bar{1}00]$ directions. As can be seen from the figure, the spacing between adatom sites alternates between a long and a short spacing along the $[1\bar{1}00]$ direction. This alternation gives rise to the pairing effect seen in the STM image. Corresponding unit cells are drawn on both the STM image and on the model for comparison.

4. Theory

Total energy calculations have been performed within the local density functional theory using first-principles pseudopotential methods for a number of possible GaN(0001) surface structures [13]. The calculations have been performed with a plane wave cut-off of 60 Ry and with the Ga 3d states included in the valence band. To sample the Brillouin zone, two special k-points have been employed for structures with C_{3v} symmetry and an equivalent set for structures having a reduced symmetry. We employ unit cells containing eight layers of GaN and relax the top four layers in addition to the adatoms. The N dangling bonds on the $[000\bar{1}]$ side of the slab are saturated by fractionally charged H atoms. The relative stability of possible structures is determined within the thermodynamically allowed range of the Ga chemical potential: $\mu_{\text{Ga(bulk)}} - \Delta H < \mu_{\text{Ga}} < \mu_{\text{Ga(bulk)}}$. The maximum chemical potential of Ga is the energy per atom of bulk Ga: $\mu_{\text{Ga(bulk)}}$. The minimum chemical potential of Ga is $\mu_{\text{Ga(bulk)}} - \Delta H$, where ΔH is the heat of formation of GaN. Our calculations indicate that ΔH is equal to 0.9 eV, in good agreement with the experimental value; 1.1 eV. The chemical potential dependence of the GaN surface energy for various structures has been discussed previously [13]. Here, we will provide additional information about the atomic structure for the low-energy structures on the (0001) surface, and make a few conjectures pertaining to possible models for the 5×5 reconstruction.

For the (0001) surface, calculations of the stability of possible models indicate that a 2×2 N adatom structure could be stable under very N-rich conditions [13]. Of all the structures examined to date, it is the most stable under N-rich conditions. In this structure, each N adatom is bonded to three Ga atoms residing in the outer part of the Ga–N bilayer. In each 2×2 cell, there is one N adatom and one Ga rest atom. The Ga rest atom transfers electrons to the N adatom, and the structure is semiconducting. A schematic representation of the structure is shown in Fig. 11. The length of the bond between the N adatom and the Ga atoms is 2.01 Å, about 4% longer than Ga–N bond in the bulk (1.94 Å). The vertical height of the N adatom is 1.15 Å above the plane defined by its three Ga neighbors. The N adatom adopts a p^3 bonding configuration, making $\sim 90^\circ$ bond angles with the underlying Ga atoms. Achieving this coordination while preserving an approximately bulk-like bond length between the adatom and the Ga atoms requires a very large relaxation of the Ga atoms. The three Ga atoms relax laterally, towards the H3 position, by 0.19 Å and move vertically (towards the adatom) by 0.24 Å. The Ga rest atom moves inwards by 0.35 Å. Thus, the vertical buckling of the Ga plane is ~ 0.6 Å. This is about 90% of the vertical separation of neighboring (0001) planes in bulk GaN.

The N adatom prefers the H3 site instead of the T4 site by a large amount: about 0.7 eV/(2×2 cell). A qualitatively similar result was obtained

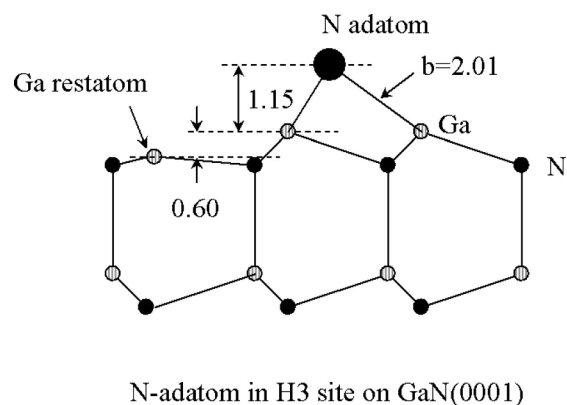


Fig. 11. Schematic model of nitrogen H3 adatom structure. All dimensions are given in angstroms.

for the N adatom on the AlN surface where the energy difference is $3.3 \text{ eV}/(2 \times 2 \text{ cell})$ [20]. The clear preference for the H3 site over the T4 site has been attributed to large electrostatic repulsion between the negatively charged N adatom and the N atom in the second layer. This repulsion is largest when the N adatom occupies the T4 site, directly above the second layer N atom [20,21]. In the N–H3 adatom structure, we expect a large tensile stress due to the N adatoms. The evidence for this stress is the fact that the Ga–N bond length (2.01 \AA) is larger than the bulk bond length (1.94 \AA). A smaller in-plane lattice constant would enable the Ga–N bond length to approach the bulk value without inducing large strains in the underlying layers. It is possible that the 5×5 structure forms in order to relieve this stress by incorporating Ga adatoms and Ga vacancies in the cell. These latter structures are not expected to be under a large tensile stress.

The Ga vacancy structure may be formed from the N adatom structure by removal of one N adatom and one Ga atom from each 2×2 cell. Thus, the two structures have the same stoichiometry, and the difference in their formation energies is independent of the atomic chemical potential. Our calculations show that the 2×2 Ga vacancy reconstruction is $0.15 \text{ eV}/(2 \times 2 \text{ cell})$ higher in energy than the N–H3 adatom structure, but in view of the small value of the energy difference, it is conceivable that the vacancy can still play a role on the GaN(0001) surface. In the vacancy reconstruction, there are equal numbers of threefold Ga and N atoms. The electrons in the Ga dangling bonds empty into the N dangling bonds and consequently the Ga atoms relax inwards towards an sp^2 bonding configuration. This results in a contraction of the Ga–N bond lengths at the surface, as shown in Fig. 12. The bond length between threefold coordinated atoms is contracted by about 4% compared to the bulk bond length, and the vertical separation of the top layer Ga and the second layer N decreases to 45% of the bulk separation. The contraction of the bond between the threefold Ga and threefold N atoms is qualitatively similar to that found on the GaN(10 $\bar{1}$ 0) surface, where a 6% contraction was calculated [22]. Note that the bond between the surface Ga and the second layer N atoms that are fourfold-

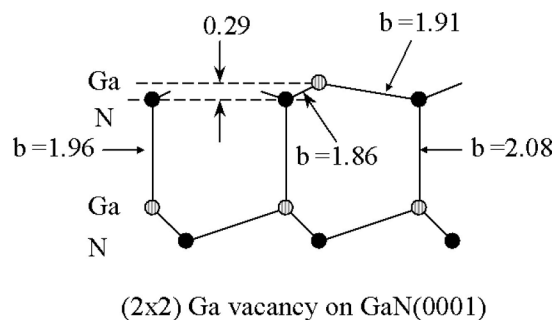


Fig. 12. Schematic model of gallium vacancy structure. All dimensions are given in angstroms.

coordinated is also contracted, but by a lesser amount (about 2%), and that the longitudinal bond between the second and third layer atoms are expanded.

The local disorder observed in the STM images of the 5×5 structure appears to suggest that there is only a weak interaction between structural sub-units that comprise the structure. One possibility for a structure built up out of weakly interacting units is a mixture of two N–H3 adatoms, one Ga–T4 adatom, and three Ga vacancies. In a 5×5 cell, such a mixture would come close to satisfying the electron counting rule, with the excess $3/4$ electron in each 5×5 cell occupying Ga dangling bonds. It is possible that a mixture of adatoms and vacancies would be stabilized by a stress-relief mechanism. As discussed above, we expect the energy of N–H3 adatom structure to be reduced by a local contraction of the surface lattice constant. This local contraction around the N adatoms could be accomplished by including Ga vacancies and adatoms in the cell. The viability of this mechanism requires that the energy of the Ga vacancy and adatom structures would be reduced, or at least not increased, by a local expansion of the surface lattice constant. Because of the small energy difference between the adatom and vacancy structures, a mixture of the two could be more stable than either structure itself. A possible arrangement of N adatoms, Ga adatoms and Ga vacancies giving rise to a 5×5 cell is indicated in Fig. 13. We note that this is a relatively open structure; convolution with an STM probe tip shape would tend to emphasize the adatoms height and diminish

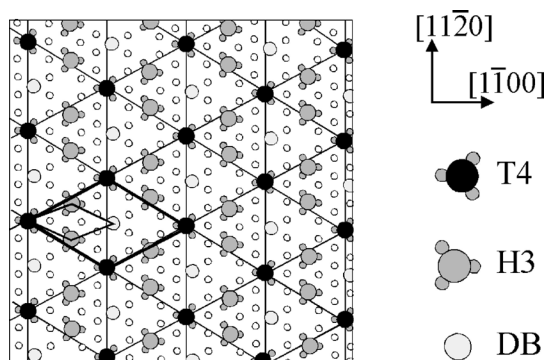


Fig. 13. Structural model for the 5×5 reconstruction. Ga adatoms in T4 sites and N adatoms in H3 sites are shown by large black and large gray circles, respectively. The small open circles in the diagram represent the Ga rest atoms in the second layer. In the locations where the small open circles are missing, Ga vacancies occur. The N atoms in the third layer are not shown. The light-gray circle labelled DB (dangling bond) is a particular Ga rest atom site. In an alternative model, this site could conceivably contain another adatom in a nearby T4 or H3 site.

the presence of the holes created by the vacancies, thus making the average surface height appear relatively large. In contrast, the structure formed in the 6×4 reconstruction, may be more closed and compact. It would then appear in STM to be *lower* than the 5×5 , while still containing more Ga atoms (and nominally the same amount of N atoms) than the 5×5 , in agreement with the observations of Section 3.2.

The other structure having a 2×2 symmetry that we find to be stable under more Ga-rich conditions is the Ga adatom. The calculations indicate that the Ga adatom prefers the T4 site over the H3 site, but by only about $0.12 \text{ eV}/(2 \times 2 \text{ cell})$. In the T4 site, the vertical height of the Ga adatom is 1.66 \AA above the bulk Ga plane, and the Ga–Ga bond length is 2.46 \AA (see Fig. 14). In the H3 site, the vertical height is 1.63 \AA above the bulk Ga plane, and the Ga–Ga bond length is 2.48 \AA (see Fig. 15). The relatively small energy difference between the two adsorption sites is a consequence of the fact that the surface Ga–Ga bonds are non-polar. Thus, the Ga adatom is charge-neutral on the (0001) surface, and does not experience a large electrostatic attraction to the second-layer N atoms. Given that the 2×2 structure seen in experiments is formed by nitridation

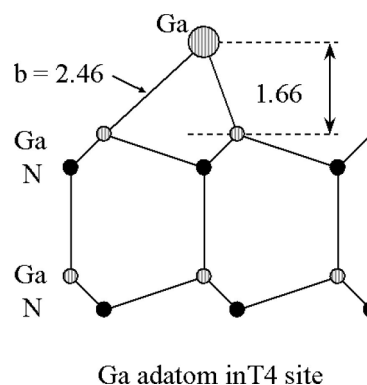


Fig. 14. Schematic model of gallium T4 adatom structure. All dimensions are given in angstroms.

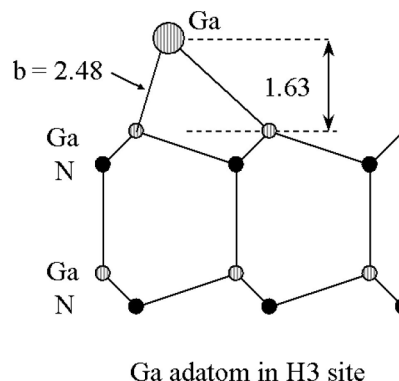


Fig. 15. Schematic model of gallium H3 adatom structure. All dimensions are given in angstroms.

[15], it seems most likely that it corresponds to the N-adatom model. However, the nitridation could be converting the surface from a Ga-rich structure to a less Ga-rich structure, with the 2×2 being the Ga adatom.

5. Conclusions

We have studied the surface reconstructions which occur on the GaN(0001) surface using a combination of experimental and theoretical techniques. We have found a family of reconstructions, including 2×2 , 5×5 , 6×4 , and ' 1×1 '. We have successfully imaged the 2×2 only in filled states; therefore, this surface appears to be semiconducting in nature. We believe this 2×2 is most consis-

tent with the N-adatom (H3) 2×2 predicted by our first-principles total energy calculations [13]. Our calculations indicate that the 2×2 N–H3 adatom model is semiconducting and that it is slightly lower in energy than the Ga-vacancy model. Based on the fact that the 2×2 is formed by nitridation and that it is difficult to image the surface by tunneling into the empty states, we believe that the N-adatom model is more likely to be correct than the Ga-adatom model. For the latter model, tunneling into empty Ga adatom dangling bond states should occur readily. With increasing Ga coverage, the 5×5 and 6×4 structures are formed. These also appear to be semiconducting, based on their very strong bias dependence, as seen in the STM images. For these two, we have identified their basic structural building blocks through a detailed analysis of the empty and filled states STM images. Structural models for the 5×5 and the 6×4 could be of the adatom/vacancy type. Whatever the correct models for the 5×5 and 6×4 , since the surfaces are semiconducting in nature, we expect the number of excess electrons or holes to be small, and the electron counting rule to be satisfied approximately. In the case of the ' 1×1 ', the surface is found to be highly metallic with fluid-like properties at room temperature. We have observed that the step edges of ' 1×1 ' terraces typically show evidence for the nucleation of a fifth type of reconstruction on the Ga face, which may indicate either a freezing out of the fluidic state or the stabilization of the fluidic state via additional Ga adatoms. A large domain of this novel structure has been found and its unusual symmetry identified as $5.08 \times 2.54\text{-R}20^\circ$. This structure is consistent with a simple adatom model having 6×3 symmetry, in the framework of a contracted and rotated primitive lattice. This observation is consistent with the conclusion, based on prior studies [16], that the ' 1×1 ' is a discommensurate fluid phase.

Acknowledgements

The authors acknowledge the contributions of V. Ramachandran for help with substrate preparation and film characterization. This work was supported by the Office of Naval Research under grant N00014-96-1-0214.

References

- [1] M.M. Sung, J. Ahn, V. Bykov, J.W. Rabalais, D.D. Koleske, A.E. Wickenden, *Phys. Rev. B* 54 (1996) 14652.
- [2] J. Ahn, M.M. Sung, J.W. Rabalais, D.D. Koleske, A.E. Wickenden, *J. Chem. Phys.* 107 (1997) 9577.
- [3] M.A. Khan, J.N. Kuznia, D.T. Olson, R. Kaplan, *J. Appl. Phys.* 73 (1993) 3108.
- [4] W.C. Hughes, W.H. Rowland, M.A.L. Johnson, J.W. Cook, J.F. Schetzina, J. Ren, J.A. Edmond, *J. Vac. Sci. Technol. B* 13 (1995) 1571.
- [5] M.E. Lin, S. Strite, A. Agarwal, A. Salvador, G.L. Zhou, N. Teraguchi, A. Rockett, H. Morkoç, *Appl. Phys. Lett.* 62 (1993) 702.
- [6] K. Iwata, H. Asahi, S.J. Yu, K. Asami, H. Fujita, M. Fushida, S. Gonda, *Jpn. J. Appl. Phys.* 35 (1996) L289.
- [7] P. Hacke, G. Feuillet, H. Okumura, S. Yoshida, *Appl. Phys. Lett.* 69 (1996) 2507.
- [8] W.S. Wong, N.Y. Li, H.K. Dong, F. Deng, S.S. Lau, C.W. Tu, J. Hays, S. Bidnyk, J.J. Song, *J. Crystal Growth* 164 (1996) 159.
- [9] R.J. Molnar, R. Singh, T.D. Moustakas, *J. Electron. Mater.* 24 (1995) 275.
- [10] E.S. Hellman, C.D. Brandle, L.F. Schneemeyer, D. Wiesmann, I. Brener, T. Siegrist, G.W. Berkstresser, D.N.E. Buchanan, E.H. Hartford, *MRS Internet J. Nitride Semicond. Res.* 1 (1996) 1.
- [11] A.R. Smith, R.M. Feenstra, D.W. Greve, M.-S. Shih, M. Skowronski, J. Neugebauer, J.E. Northrup, *Appl. Phys. Lett.* 72 (1998) 2114.
- [12] A.R. Smith, V. Ramachandran, R.M. Feenstra, D.W. Greve, M.-S. Shin, M. Skowronski, J. Neugebauer, J.E. Northrup, *J. Vac. Sci. Technol. A* 16 (1998) 1641.
- [13] A.R. Smith, R.M. Feenstra, D.W. Greve, J. Neugebauer, J.E. Northrup, *Phys. Rev. Lett.* 79 (1997) 3934.
- [14] A.R. Smith, R.M. Feenstra, D.W. Greve, J. Neugebauer, J.E. Northrup, *Appl. Phys. A* 66 (1998) S947.
- [15] A.R. Smith, R.M. Feenstra, D.W. Greve, A. Ptak, T.H. Myers, T.H. Myers, W. Sarney, L. Salamanca-Riba, M.-S. Shin, M. Skowronski, *MRS Internet J. Nitride Semicond. Res.* 3 (1998) 12.
- [16] A.R. Smith, R.M. Feenstra, D.W. Greve, M.-S. Shin, M. Skowronski, J. Neugebauer, J.E. Northrup, *J. Vac. Sci. Technol. B* 16 (1998) 2242.
- [17] F.A. Ponce, D.P. Bour, W.T. Young, M. Saunders, J.W. Steeds, *Appl. Phys. Lett.* 69 (1996) 337.
- [18] B. Daudin, J.L. Rouvière, M. Arlery, *Appl. Phys. Lett.* 69 (1996) 2480.
- [19] J.L. Rouvière, M. Arlery, R. Niebuhr, K.H. Bachem, O. Briot, *MRS Internet J. Nitride Semicond. Res.* 1 (1996) 33.
- [20] J.E. Northrup, R. Di Felice, J. Neugebauer, *Phys. Rev. B* 55 (1997) 13878.
- [21] K. Rapcewicz, M.B. Nardelli, J. Bernholc, *Phys. Rev. B* 56 (1997) R15725.
- [22] J.E. Northrup, J. Neugebauer, *Phys. Rev. B* 53 (1996) 10477.